Acta Crystallographica Section A
Foundations of Crystallography
ISSN 0108-7673

Received 17 June 2009
Accepted 17 September 2009

This study is dedicated to the late Professor Lubor Žák (29 July 1925 – 6 August 2008), a discoverer of the species

The OD interpretation of the crystal structure of kettnerite $CaBiOFCO_3$

Jiří Hybler[a]* and Slavomil Ďurovič[b]

[a]Institute of Physics, Academy of Sciences of the Czech Republic, Na Slovance 2, CZ-18221, Praha 8, Czech Republic, and [b]Institute of Inorganic Chemistry, Slovak Academy of Sciences, SK-84236 Bratislava, Slovakia. Correspondence e-mail: hybler@fzu.cz

The mineral kettnerite, $CaBi(OFCO_3)$, is a rare example of an order–disorder (OD) structure with a quadratic net. The lattice parameters of the simplest possible 1*O* polytype are $a = 5.3641$ (1), $b = 5.3641$ (1), $c = 13.5771$ (2) Å, and the space group is *Pbaa*. There are three kinds of OD layers, identical to structure-building layers. Two of them are non-polar: the Bi—O and Ca—F at $z = 0$ and $z = 1/2$, respectively, with the layer-group symmetry $C2/m2/m(4/a,b)2_1/m2_1/m$. The third kind of OD layer of CO_3 groups (located between the Bi—O and Ca—F layers) is polar, with alternating sense of polarity. The layer group is *Pba*(4)*mm*. Triangular CO_3 groups are parallel to (110) or $(1\bar{1}0)$ planes with one O atom oriented towards the Bi—O layer and the remaining two O atoms oriented towards the Ca—F layer. The orientations of CO_3 groups alternate along the [110] and $[1\bar{1}0]$ directions. As a result, each group parallel to (110) is surrounded by four nearest neighbors parallel to $(1\bar{1}0)$ and *vice versa*. These positions can be interchanged by an $(\mathbf{a} + \mathbf{b})/2$ shift or by $\pi/2$ rotation; thus stacking of the layer onto adjacent ones is ambiguous. Instead of OD layers, the polytypes are generated by stacking of OD packets, comprising the whole CO_3 layers and adjacent halves of the Bi—O and Ca—F layers. They are polar, with alternating sense of polarity; the layer group is *Pba*(4)*mm*. Stacking sequences are expressed by ball-and-stick models, with the aid of symbolic figures, and by sequences of orientational characters. There are two maximum-degree-of-order (MDO) polytypes, 1*O* (really found and described, see lattice parameters and space group above) and 2*O*, with doubled *c* parameter and space group *Ibca* (not yet found). The derivation of the MDO generating operations of both polytypes is presented in this paper. The stacking rule also allows another, non-MDO, polytype with doubled *c*, *i.e.* the 2*Q* polytype, space group $P4_2bc$ (tetragonal, not yet found). Various kinds of domains can exist: (i) out-of-step domains shifted by $(\mathbf{a} + \mathbf{b})/2$, (ii) twin domains rotated by $\pi/2$ around local tetrads of odd or even packets, and (iii) upside-down domains in the polar 2*Q* polytype. Stacking sequences of 16 possible domains of the polytypes mentioned above are listed. Also 60 domains of four distinct six-packet polytypes are theoretically possible.

1. Introduction

The mineral kettnerite $CaBi[OFCO_3]$ has been found in Krupka, Krušné hory (Ore Mountains), NW Bohemia, and described by Žák & Syneček (1956, 1957). The first structure determination by Syneček & Žák (1960) provided positions of all atoms except those belonging to CO_3 groups. The arrangement of these groups remained undetermined for a long time, and it was also unclear whether the structure should be described in the smaller tetragonal cell ($a \simeq 3.8$ Å, $c \simeq 13.6$ Å) or in a larger supercell. Recently, Hybler & Dušek (2007) have revealed the existence of weak and diffusely streaked superlattice (in fact polytype) diffraction spots justifying the description of the structure in the supercell $a = 5.3641$ (1), $b = 5.3641$ (1), $c = 13.5771$ (2) Å. Although the unit cell is metrically tetragonal, the structure was refined in the orthorhombic space group *Pbaa*.

The structure (Fig. 1) is built up of three kinds of building layers parallel to (001). The first one contains O1 atoms in a square array at $z = 0$ and two adjacent planes of Bi atoms facing the centers of the squares (Bi—O layers). This kind of layer has also been found in the minerals bismutite $Bi_2O_2CO_3$ and beyerite $CaBi_2O_2(CO_3)_2$ (Lagercrantz & Sillén, 1948) as well as in Aurivillius phases (Aurivillius, 1949*a*,*b*, 1950). A similar layer of F1 atoms is located at $z = 1/2$ with two adjacent planes of Ca atoms (Ca—F layers). Both these layers are

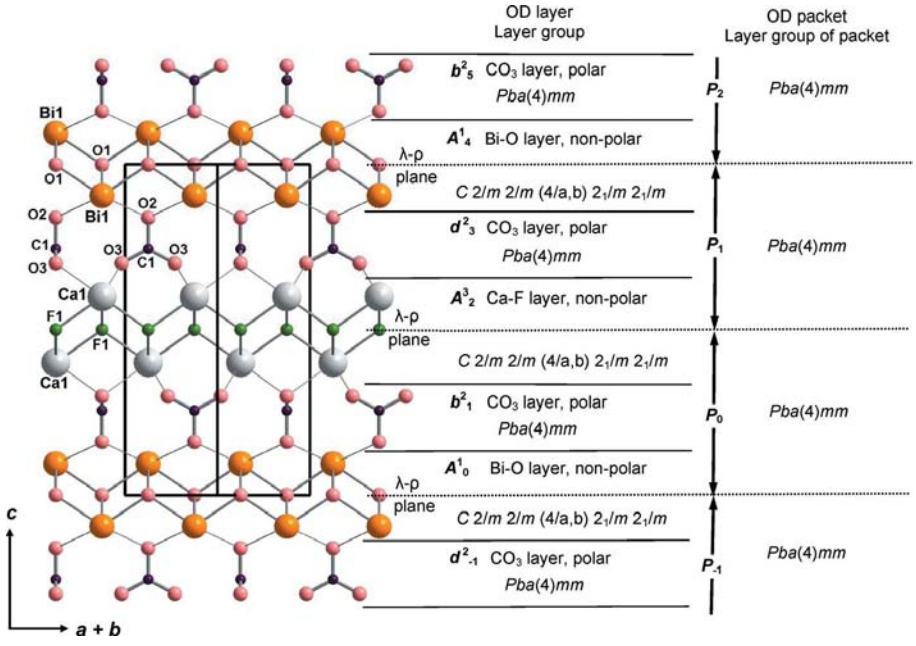

Figure 1
Crystal structure of kettnerite (idealized): a slice parallel to the $(1\bar{1}0)$ plane of the larger cell. OD layers and packets are indicated.

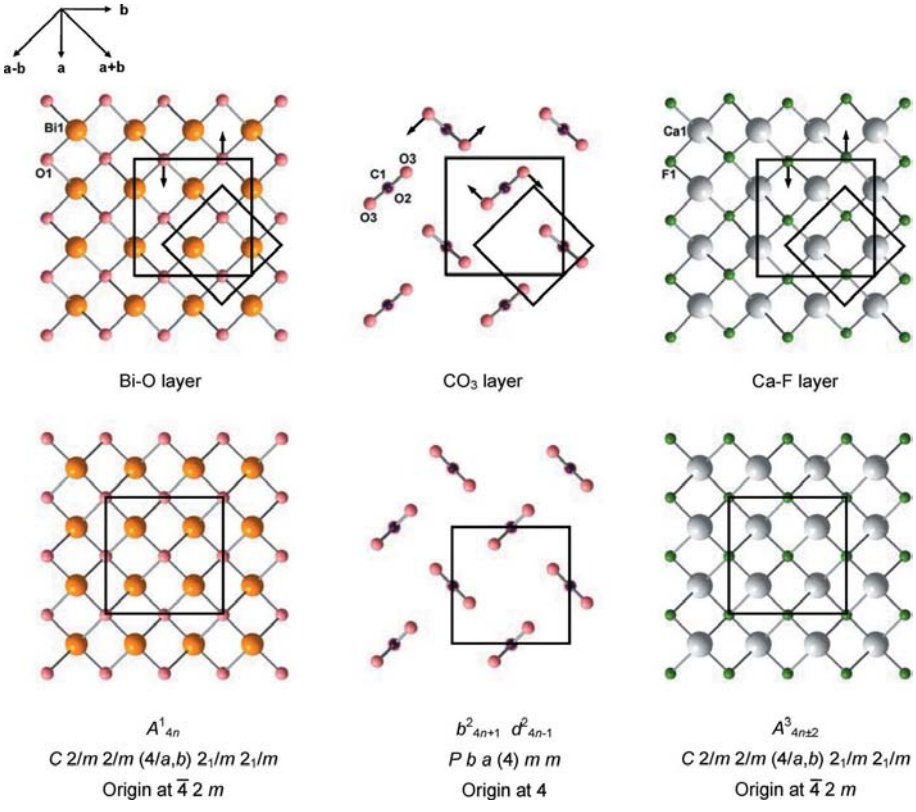

Figure 2
Top: structure-building layers of kettnerite, projection down **c**. The smaller and larger cells are indicated. Displacements of atoms owing to desymmetrization are indicated by arrows. Bottom: corresponding OD layers, idealized model. Unit cells are chosen with respect to the layer groups indicated below.

pseudotetragonal with the periodicity corresponding to the **a** and **b** vectors of the smaller cell. The layers of CO_3 groups are located between Bi—O and Ca—F layers. The triangular CO_3 groups are oriented close to the (110) or $(1\bar{1}0)$ planes, with (apical) O2 atoms pointing towards the Bi—O layer, while the remaining pairs of (basal) O3 atoms are oriented towards the Ca—F layer. The orientations of CO_3 groups alternate in two directions, along [110] and $[1\bar{1}0]$, so that each group close to (110) is surrounded by four nearest neighbors close to $(1\bar{1}0)$ and *vice versa* [*cf.* Fig. 2 (top)]. This structure model provides reasonable distances of equally charged O3 atoms, but it requires description of the structure in the larger supercell. The orientation of every CO_3 group (and consequently of all their neighbors, and neighbors of neighbors *etc.*) can be mutually interchanged. This interchange can also be interpreted as a shift of the whole CO_3 layer along the (**a** + **b**)/2 vector (of the larger supercell) or $\pi/2$ rotation of the layer. This ambiguity in the stacking of the CO_3 layer causes the order–disorder (OD) character of kettnerite.

The structure determination based on the subset of reflections corresponding to the smaller cell ($h + k = 2n$ in the large supercell indexing) produces a tetragonal *family structure*, in which both possible positions of the triangular CO_3 group interpenetrate, forming a peculiar square pyramid. In this pyramid the O2 atom is on the apex while four half-occupied O3 atoms form the base. Since all heavy (and some light) atoms are in special positions obeying the symmetry of the family structure, they do not contribute to polytype reflections. The latter reflections are produced by O3 atoms and also by small contributions from O1 and F1 atoms, misplaced from ideal positions owing to desymmetrization (Ďurovič, 1979). As a consequence, the polytype reflections are very weak, and they are further weakened or even disappear owing to various degrees of disorder. This fact considerably obstructed the correct structure determination.

The structure has been described in detail in a previous paper (Hybler & Dušek, 2007). However, its OD character was only briefly mentioned. Since kettnerite represents a kind of an OD structure with a quadratic net, not observed as yet, it is worth describing it in detail. The aim of this paper is to present a thorough description, as well as the derivation, of maximum-degree-of-order (MDO) and of some non-MDO polytypes allowed by the stacking rule.

2. Terms and conventions

It seems proper to recall some important properties of OD structures. They consist of OD layers, three-dimensional objects with two-dimensional periodicity, not necessarily identical to crystal chemical building layers. The OD layers are related by partial coincidence operations, denoted as POs in the following. The POs converting a layer into itself are called λ-POs; those converting an OD layer into an adjacent one are called σ-POs. The ensemble of λ-POs of the given layer constitutes one of 80 possible layer groups (Dornberger-Schiff, 1956). POs not changing the orientation of the layer are denoted as τ-POs; those turning the layer upside down are called ρ-POs. Both λ- and σ-POs can be, depending on the category of the OD structure, either τ or ρ. Of 80 layer groups, 17 are polar, containing the τ-POs only, the remaining 63 are non-polar, containing both λ- and σ-POs. The layer groups are described by Hermann–Mauguin symbols, where the direction of lacking periodicity is indicated in parentheses. For quadratic nets, like in the case of kettnerite, the full five-entry symbols of layer groups related to all important directions **a**, **b**, **c**, **a** + **b** and **a** − **b** (in the given order) are often used, like, for example, *P b a* (4) *m m* (Dornberger-Schiff, 1956, 1964, 1966). The main property of OD layers is their stacking ambiguity, which means that there is always more than one possibility as to how the consecutive layers can be stacked.

3. Idealized model of the structure of kettnerite

In order to simplify the description of the structure and derivation of polytypes, the idealized structure model neglecting the desymmetrization is used throughout this study. This model assumes 'perfectly diagonal' orientation of CO_3 groups parallel to (110) or (1$\bar{1}$0) planes, and F1 and O1 atoms in special positions at $\bar{4}$, not displaced as in the real structure (Hybler & Dušek, 2007). The deviations from the ideal model can be mentioned and discussed when necessary.

In this study, all translational components of POs will be related to the vectors **a**, **b**, of the larger cell, and the repeat unit $\mathbf{c}_0$, identical to the **c** vector of the family structure.

3.1. OD layers

The structure belongs to the category IV OD structures composed of more than one kind of layer (Dornberger-Schiff & Grell, 1982; Ďurovič, 1997, 1999). In our case we can distinguish three kinds of layers; two of them are non-polar, and the remaining one is polar, appearing in the structure with alternating sense of polarity (Fig. 2).

OD layers are defined as follows (*cf.* Hybler & Dušek, 2007):

(i) $A^1{}_{4n}$ OD layer (denoted Bi—O layer in the following), comprising the plane of O1 atoms at $z = 0$, and two adjacent planes of Bi1 atoms at $z = \pm 0.094$, symmetry $C(4/a)mm$ (shortened symbol) or $C\ 2/m\ 2/m\ (4/a,b)\ 2_1/m\ 2_1/m$ (full five-entry symbol). The multiplicity of the layer group is 32 (16τ + 16ρ POs). The origin of the layer is set at $\bar{4}2m$. The layer is non-polar. The layer-group symbols are related to the vectors of the larger supercell, while the layer itself is periodic with respect to the smaller subcell. As a consequence, the unusual symbol with a *C*-centering appears. The layer-group symbols related to vectors of the smaller cell read: $P\ 2_1/m\ 2_1/m\ (4/n)\ 2/m\ 2/m$ (full five-entry symbol) and $P(4/n)mm$ (shortened symbol). There is one λ–ρ plane corresponding to the plane of O1 atoms.

(ii) $b^2{}_{4n+1}$ and $d^2{}_{4n-1}$ OD layers (denoted as CO_3 layers in the following), comprising C1 atoms at $z = 0.256$, O2 atoms at $z = 0.161$ and pairs of O3 atoms at $z = 0.299$. The shortened and full (five-entry) layer-group symbols are $P(4)bm$ and $Pba(4)mm$, respectively. The origin of the layer is at (4). The layers are polar, with regularly alternating sense of polarity. The polarity of b_{4n+1} is opposite to that of d_{4n-1}. The general multiplicity of the group is 8 (τ operations only). The translation group of $b^2{}_{4n+1}$ and $d^2{}_{4n-1}$ is a subgroup of translation group of $A^1{}_{4n}$ and $A^3{}_{4n\pm2}$ and the layer is periodic with respect to **a** and **b** vectors of the larger supercell.

(iii) $A^3{}_{4n\pm2}$ OD layer (denoted as Ca—F layer in the following), comprising the plane of F1 atoms at $z = 1/2$ and two adjacent planes of Ca1 atoms at $z = 1/2 \pm 0.1$. The layer symmetry is the same as that of the $A^1{}_{4n}$ (Bi—O layer), $C(4/a)mm$ (shortened symbol) or $C\ 2/m\ 2/m\ (4/a,b)\ 2_1/m\ 2_1/m$ (full five-entry symbol). The origin is set at $\bar{4}2m$. The layer is non-polar. The *C*-centering is used for the same reason as in the case of the Bi—O layer. There is one λ–ρ plane corresponding to the plane of F1 atoms.

There is one Bi—O, one Ca—F and two CO_3 (of opposite polarities) OD layers per repeat unit $\mathbf{c}_0$. It should be emphasized that the choice of OD layers in OD structures of category IV of more than one kind of layer is not unique and interlayer boundaries can be set in more than one way. For instance, the half or the whole O2 atom or even the C1 atom can be appended to the Bi—O layer instead of to the CO_3 layer. The described choice of OD layers is thus one of several possible ones. It is used in this study because of its closeness to crystal chemical building layers. The projections of OD layers down **c** in the idealized model are shown in Fig. 2 (bottom). The choice of OD layers is also indicated on the right-hand side of Fig. 1. There are two kinds of layer pairs: (Bi—O; CO_3), (CO_3; Ca—F).

For the given category of OD structures the symbol of the OD groupoid family consists of two lines. In the first line there are symbols of layer groups of the consecutive layers; their sequence starts and ends with the symbols of non-polar layers. In the second line there are, in square brackets, components of

Table 1
NFZ relation for OD layers of the kettnerite family.

OD layer		Layer group	N	F	Z
$A^1{}_0$	Bi—O	$C\,2/m\,2/m\,(4/a,b)\,2_1/m\,2_1/m$	16	8	2
$b^2{}_1$	CO_3	$Pba(4)mm$	8	8	1
$A^3{}_2$	Ca—F	$C\,2/m\,2/m\,(4/a,b)\,2_1/m\,2_1/m$	16	8	2
$d^2{}_3$	CO_3	$Pba(4)mm$	8	8	1
$A^1{}_4$	Bi—O	$C\,2/m\,2/m\,(4/a,b)\,2_1/m\,2_1/m$	16	8	2
$b^2{}_5$	CO_3	$Pba(4)mm$	8		

shifts of origins of the layer (as defined above) with respect to the origin of the preceding layer (Grell & Dornberger-Schiff, 1982; Ďurovič, 1997).

The symbol of the OD groupoid family of kettnerite thus reads

$$\underset{\left[+\frac{1}{4},+\frac{1}{4}\right]}{C2/m2/m(4/a,b)2_1/m2_1/m}\quad \underset{\left[-\frac{1}{4},-\frac{1}{4}\right]}{Pba(4)mm}\quad \underset{\left[-\frac{1}{4},-\frac{1}{4}\right]}{C2/m2/m(4/a,b)2_1/m2_1/m}$$

or, in the shortened form,

$$\underset{\left[+\frac{1}{4},+\frac{1}{4}\right]}{C(4/a)mm}\qquad \underset{\left[-\frac{1}{4},-\frac{1}{4}\right]}{P(4)bm}\qquad \underset{\left[-\frac{1}{4},-\frac{1}{4}\right]}{C(4/a)mm}$$

The general multiplicity of the τ subgroup of the layer group $C\,2/m\,2/m\,(4/a,b)\,2_1/m\,2_1/m$ of the $A^1{}_{4n}$ (Bi—O) layer is $N = 16$; the multiplicity of the layer group $Pba(4)mm$ of $b^2{}_{4n+1}$ or $d^2{}_{4n-1}$ (CO_3) layers is 8. The general multiplicity of the τ subgroup of operations valid for the layer pair ($A^1{}_{4n}$; $b^2{}_{4n+1}$) is $F = 8$. The *NFZ* relation (Dornberger-Schiff, 1964) reads $Z = N/F = 16/8 = 2$. There are thus two possibilities as to how the $b^2{}_{4n+1}$ (CO_3) layer can be stacked onto the $A^1{}_{4n}$ (Bi—O) layer. Analogously, the same relation is valid for the ($A^1{}_{4n}$; $d^2{}_{4n-1}$) layer pair (Bi—O layer + CO_3 layer attached at the opposite side), as well as for both possible pairs of Ca—F and CO_3 layers ($A^3{}_{4n\pm2}$; $b^2{}_{4n+1}$) and ($A^3{}_{4n\pm2}$; $d^2{}_{4n-1}$). The *NFZ* relations are summarized in Table 1.

3.2. OD packets, symbolic figures

For OD structures of more kinds of layers the derivation of MDO (but also other periodic) polytypes is a complicated task because of the different geometry of OD layers. It has proven useful to use structural units larger than individual OD layers, the so-called OD packets (Ďurovič, 1974). According to the definition, an OD packet is the smallest continuous part of the OD structure which is periodical in two dimensions and which represents completely its composition. In kettnerite, the OD packet comprises the CO_3 layer + adjacent halves of the Bi—O and Ca—F layers. The packet boundaries are identical to the λ–ρ planes (*cf.* Fig. 1) and the O1 and F1 atoms are halved by them. Although the packet contains halves of Bi—O and Ca—F layers (the structure parts of higher symmetry), the symmetry of the whole packets is determined by the symmetry of the CO_3 layer, $Pba(4)mm$. The polarity and stacking ambiguity of the CO_3 layer determines the polarity and stacking ambiguity of the whole packet. Even- and odd-numbered packets are geometrically equivalent. They differ in the sense of polarity and alternate regularly in the structure. There are two packets (of opposite polarities) per repeat unit $\mathbf{c}_0$.

Similarly to CO_3 layers, every packet can appear in two possible positions shifted from each other by $(\mathbf{a} + \mathbf{b})/2$. Using the packets instead of layers, kettnerite can be *formally* handled as an OD structure of one kind of layer of the category III (Ďurovič, 1997, 1999).

The symbol of the OD groupoid family for kettnerite then reads

$$\begin{array}{lllllll} P & b & a & (4) & m & m & \lambda \text{ operations within the packet,} \\ & \{2_0 & 2_1 & \left(\frac{\bar{4}}{n_{1,0}}\right) & 2_{-1/2} & 2_{1/2}\} & \sigma \text{ operations : even} \rightarrow \text{odd packet,} \\ & \{2_0 & 2_1 & \left(\frac{\bar{4}}{n_{1,0}}\right) & 2_{1/2} & 2_{-1/2}\} & \sigma \text{ operations : odd} \rightarrow \text{even packet.} \end{array}$$

There are the following λ-POs: 1, [. . (4^1) . .], [. . (4^2) . .], [. . (4^3) . .] (congruent, rotations around the fourfold axis), [. *a* (.) . .], [. . (.) . *m*], [*b* . (.) . .] and [. . (.) *m* .] (enantiomorphous, mirror and glide reflections in planes perpendicular to the packet boundary plane). The σ-POs (even-to-odd packet) are as follows: [. 2_1 (.) . .]$^+$, [2 . (.) . .]$^+$ (congruent, with reverse continuation), [. . (.) $2_{-1/2}$.]$^-$, [. . (.) . $2_{1/2}$]$^-$ (congruent, without reverse continuation), [$\bar{1}$]$^+$, [. . (*a*) . .]$^+$ (enantiomorphous, with reverse continuation) and [. . ($\bar{4}^1$) . .]$^-$, [. . ($\bar{4}^3$) . .]$^-$ (enantiomorphous, without reverse continuation). In the following, the + or − sign in the superscript indicates the σ-POs with and without reverse continuation, respectively.

It has proven useful to display OD layers or packets in the form of arrays of appropriately chosen symbolic figures rather than in the form of ball-and-stick models. Such figures preserve the symmetry of layers or packets (responsible for their stacking), ignore unnecessary structure details, and thus allow handling of the structure with a high degree of abstraction. Since the symmetry of the kettnerite packet is determined by the symmetry of the CO_3 layer (see above), only this symmetry needs to be reflected by the symbolic figures. All atoms belonging to Bi—O and Ca—F layers can thus be ignored. This approach greatly facilitates further considerations.

The symbolic figures chosen for kettnerite packets correspond to the structure motifs shown in Fig. 3, in projection

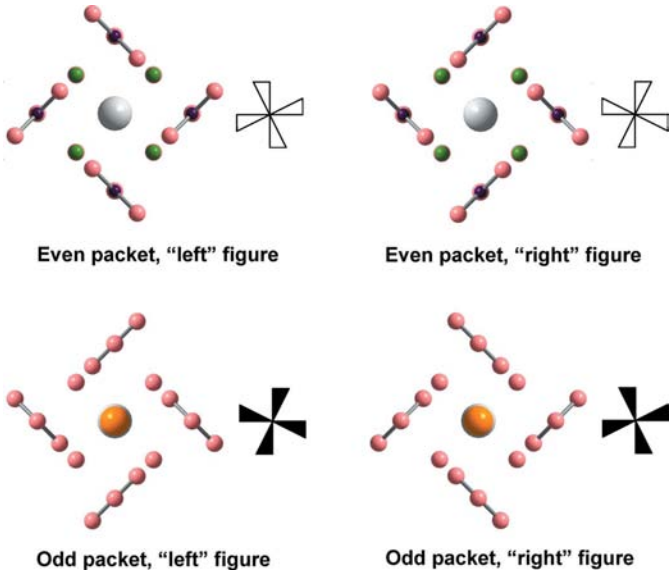

Figure 3
Arrangement of the CO_3 groups around local tetrads in the even and odd packets in projections down **c**, alongside the assigned symbolic figures.

down **c**. They have fourfold symmetry and centers in tetrads. With respect to two possible arrangements of CO_3 groups around tetrads the 'left' and 'right' figures can be distinguished. The symbolic figures of even-numbered packets denoted in the following as P_{2n} (P_0, P_2, P_4 *etc.*) are oriented to the observer by the 'white' side, while those representing the odd-numbered packets (of opposite polarity) denoted as P_{2n+1} (P_1, P_3, P_5 *etc.*) by the 'black' side. In Figs. 4(*a*) and 4(*b*) the even and odd packets are presented, partially in the ball-and-stick model and partially with the aid of symbolic figures. The superposition of one even and one odd packet [the packet pair (P_0; P_1)] is shown in Fig. 4(*c*). In the packet, every 'right' symbolic figure is surrounded by four 'left' ones (of the same color) and *vice versa*. In the projection of the packet pair, the positions of symbolic figures belonging to even and odd packets are such that every 'white' figure is surrounded by four 'black' ones, two of them are 'left', the other two are 'right'.

In pictures displaying more than two packets, the symbolic figures will be colored as follows: white for P_0, black for P_1, empty red for P_2 and full red for P_3 packets.

The positions of symmetry elements corresponding to λ-POs of a single packet (P_{2n}) are indicated in Fig. 5(*a*), while those corresponding to σ-POs of the packet pair (P_{2n}; P_{2n+1}) are shown in Fig. 5(*b*). One important property of the structure can be recognized in these (and also in the previous) pictures: the tetragonal symmetry is obeyed solely for the array of figures of the same color (*i.e.* single packet) but not for both colors simultaneously (*i.e.* packet pair). Thus the packet pair as a whole has only twofold symmetry.

As mentioned above, the layer symmetry of a single packet is determined by the symmetry of the CO_3 layer, *Pba*(4)*mm*, with general multiplicity $N = 8$. The layer group of the packet pair (P_{2n}; P_{2n+1}) is *Pba*(*a*). The general multiplicity of the τ subgroup of operations is $F = 4$. The *NFZ* relation for the packet pair reads $Z = N/F = 8/4 = 2$. There are thus two possibilities as to how the packet P_{2n+1} can be stacked onto P_{2n} and *vice versa*.

3.3. Stacking of packets

The stacking sequence in any polytype can be generally expressed as

$$\underset{v_{01}}{T_0 \bullet T_1} \quad \underset{v_{12}}{T_2 \bullet T_3} \quad \underset{v_{23}}{T_4 \bullet T_5} \quad \underset{v_{34}}{\ldots} \quad \underset{v_{45}}{T_i \bullet T_{i+1}} \quad \underset{v_{ii+1}}{} \qquad (1)$$

where T_i are orientational characters which in the present case are as follows: R and L for right and left symbolic figure, respectively, placed in the defined position. The v_{ii+1} symbols are displacement characters, corresponding to displacement

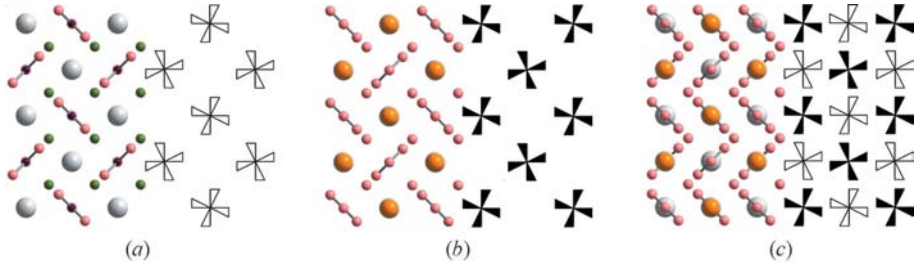

Figure 4
Even packet (*a*), odd packet (*b*) and superposition of both (*c*) in projections down **c**, in the ball-and-stick model (left) and using symbolic figures (right).

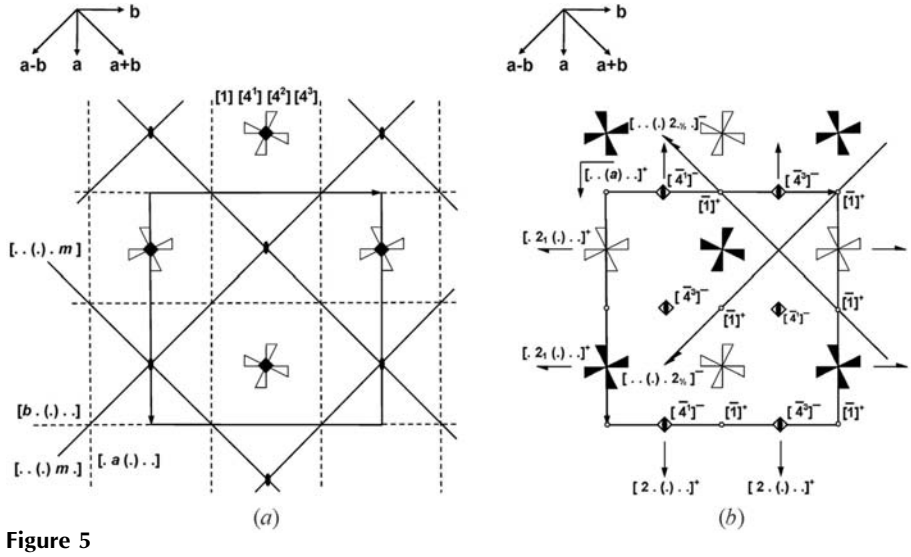

Figure 5
Set of λ-POs of one packet (*a*) and of $_{0,1}[\rho]$ POs transforming the even packet into the odd one (*b*).

Table 2
MDO1 polytype $1O$, unit cell **a**, **b**, $\mathbf{c}_0$; multiplicative table of ${}_{0,1}[\rho_1]^+ \cdot {}_{1,2}[\rho_1]^+ = {}_{0,2}[\tau]$ MDO-generating operations.

Note that z coordinates and z components of screw axes and glide planes are related to the repeat unit $\mathbf{c}_0$.

	${}_{1,2}[\rho_1]$			
${}_{0,1}[\rho_1]$	${}_{1,2}[. 2_1 (.) . .]$ $[x = 1/4, z = 1]$	${}_{1,2}[2 . (.) . .]$ $[y = 1/4, z = 1]$	${}_{1,2}[\bar{1}]$ $[x = 0, y = 0, z = 1]$	${}_{1,2}[. . (a) . .]$ $[z = 1]$
${}_{0,1}[. 2_1 (.) . .]$ $[x = 1/4, z = 1/2]$	${}_{0,2}[\boldsymbol{t}_{\mathbf{c}_0}]$	${}_{0,2}[. . 2_2 . .]$	${}_{0,2}[. n_{1,2} . . .]$	${}_{0,2}[n_{2,1} . . . .]$
${}_{0,1}[2 . (.) . .]$ $[y = 1/4, z = 1/2]$	${}_{0,2}[. . 2_2 . .]$	${}_{0,2}[\boldsymbol{t}_{\mathbf{c}_0}]$	${}_{0,2}[n_{2,1}. . . .]$	${}_{0,2}[. n_{1,2} . . .]$
${}_{0,1}[\bar{1}]$ $[x = 0\ y = 0, z = 1/2]$	${}_{0,2}[. n_{1,2} . . .]$	${}_{0,2}[n_{2,1} . . . .]$	${}_{0,2}[\boldsymbol{t}_{\mathbf{c}_0}]$	${}_{0,2}[. . 2_2 . .]$
${}_{0,1}[. . (a) . .]$ $[z = 1/2]$	${}_{0,2}[n_{2,1} . . . .]$	${}_{0,2}[. n_{1,2} . . .]$	${}_{0,2}[. . 2_2 . .]$	${}_{0,2}[\boldsymbol{t}_{\mathbf{c}_0}]$

vectors. The dot (•) above a displacement character (not necessary in some categories of OD structures) indicates the even-to-odd packet boundary, corresponding to the F atoms plane in the real structure. Because of the arrangement of white and black symbolic figures, there are four (shortest) possible displacement vectors, $+\mathbf{a}/2$, $-\mathbf{a}/2$, $+\mathbf{b}/2$ and $-\mathbf{b}/2$. These symbols of vectors may be used as displacement characters v_{ii+1}.

However, if the displacement vectors are chosen arbitrarily, the above principle allows description of the same sequence of packets in many alternative but equivalent ways. Therefore, it seems proper to adopt some additional rules for selection of displacement vectors. Thus the following possible values of v_{ii+1} are selected: $+\mathbf{a}/2$ for $i = 2n$ and $-\mathbf{a}/2$ for $i = 2n + 1$. It is also recommended to start the initial sequence of packets (not a result of some transformation) with the *right white* 'reference' symbolic figure belonging to the P_0 packet (*cf.* Fig. 5*b*, in the center of the first row from the top). The stacking sequence of the packet pair reads

$$\begin{matrix} \mathrm{R} & \bullet & \mathrm{L} \\ +\mathbf{a}/2 & & -\mathbf{a}/2 \end{matrix} \qquad (2)$$

A longer sequence can be expressed as

$$\begin{matrix} \mathrm{R} & \bullet & \mathrm{L} & \mathrm{R} & \bullet & \mathrm{L} & \mathrm{R} & \bullet & \mathrm{L} \\ +\mathbf{a}/2 & & -\mathbf{a}/2 & +\mathbf{a}/2 & & -\mathbf{a}/2 & +\mathbf{a}/2 & & -\mathbf{a}/2 \end{matrix} \qquad (3)$$

The regular alternation of $+\mathbf{a}/2$ and $-\mathbf{a}/2$ displacement vectors results in the zig-zag arrangement of figures. Therefore, all 'reference' figures of P_{2n} and of P_{2n+1} packets are always superimposed with the 'reference' figures of P_0 and P_1, respectively. The orientational character for the reference figure (R or L) determines unambiguously one of two possible positions of each packet.

The expression of the stacking sequence can be further simplified. Since the sequence of displacement vectors is always $+\mathbf{a}/2\ -\mathbf{a}/2\ +\mathbf{a}/2\ -\mathbf{a}/2\ +\mathbf{a}/2\ \ldots$ *etc.*, it is unnecessary to repeat it again and again. Moreover, every kind of displacement vector belongs to the given kind of packet boundary: the dot (•) and the empty space ( ) always indicate $+\mathbf{a}/2$ and $-\mathbf{a}/2$ shifts, respectively. Keeping this fact in mind, the displacement characters can be omitted, and the whole sequence can be expressed by a one-line symbol, such as

$$\mathrm{R} \bullet \mathrm{L} \quad \mathrm{R} \bullet \mathrm{L} \quad \mathrm{R} \bullet \mathrm{L}. \qquad (4)$$

These simplified expressions of sequences of packets will be used in the following.

3.4. MDO polytypes

Any family of polytypes theoretically contains an infinite number of periodic and non-periodic structures. However, periodic polytypes can be subdivided into two groups, the 'privileged' polytypes and the remaining ones. These privileged polytypes are named as basic, standard, simple or regular. They represent the simplest possible sequences of layers (or packets) and usually belong to the most frequently occurring ones. The OD theory pays special attention to polytypes in which all layer triples, quadruples *etc.* are geometrically equivalent, or, at least, which contain the smallest possible number of kinds of these units. They are called MDO (maximum degree of order) polytypes (Dornberger-Schiff, 1964, 1966; Ďurovič, 1997, 1999). For every MDO polytype there exists (one or more than one) τ-PO with translational component parallel with the stacking direction, with magnitude equal to the distance between two τ-equivalent layers (packets). This PO is called a *generating operation* and the structure of the given polytype is derived by its repetition. As the generating operation becomes total, it is also contained in the space group of the polytype. The possible MDO polytypes of kettnerite are described in this article.

The procedure for derivation of MDO polytypes was described, for example, by Weiss & Ďurovič (1980) for Mg-vermiculite (*cf.* Dornberger-Schiff & Grell, 1982). In a slightly modified form it is now applied to kettnerite:

(i) Take a starting OD packet P_0 of one kind.

(ii) Form all triples of equivalent packets (P_0; P_1; P_2) that are permitted by the stacking rule and for each one take note of all ${}_{0,1}[\rho]^+$ POs. Similarly, take note of all POs ${}_{0,1}[\rho]$ and ${}_{1,2}[\rho]$. Keep only those packet triples for which at least one ${}_{0,1}[\rho]^+$ and one ${}_{1,2}[\rho]^+$ PO exists.

(iii) For any of the packet triples selected in (ii), form all products ${}_{0,1}[\rho]^+ \cdot {}_{1,2}[\rho]^+ = {}_{0,2}[\tau]$, thus obtaining coincidence operations transforming P_0 to P_2.

(iv) Take these operations one by one and apply them on the triple (P_0; P_1; P_2) adding further packets P_4, P_5, ... in proper positions and orientations until a packet translationally equivalent to P_0 is obtained. The coincidence operation applied then becomes a total symmetry operation of the polytype in which all packet triples are equivalent and it is called an MDO-generating operation.

(v) Determine other symmetry operations thus generated, the space group of the polytype, determine basic vectors and eventually re-orient the polytype into the conventional setting.

(vi) Repeat the procedure for the remaining POs noted in (iii).

Table 3
MDO2 polytype $2O$, unit cell **a**, **b**, $2\mathbf{c}_0$; multiplicative table of ${}_{0,1}[\rho_1]^+ \cdot {}_{1,2}[\rho_2]^+ = {}_{0,2}[\tau]$ MDO-generating operations.

Note that z coordinates and z components of screw axes and glide planes are related to the repeat unit $\mathbf{c}_0$.

	${}_{1,2}[\rho_2]$			
${}_{0,1}[\rho_1]$	${}_{1,2}[2_1 \,.\, (\,.\,)\,.\,.]$ $[y = 0, z = 1]$	${}_{1,2}[.\ 2\ (\,.\,)\,.\,.]$ $[x = 1/2, z = 1]$	${}_{1,2}[\bar{1}]$ $[x = 1/4, y = 1/4, z = 1]$	${}_{1,2}[.\,.\,(b)\,.\,.]$ $[z = 1]$
${}_{0,1}[.\ 2_1\ (\,.\,)\,.\,.]$ $[x = 1/4, z = 1/2]$	${}_{0,2}[.\,.\,2_2\,.\,.]$	${}_{0,2}[\boldsymbol{t}_{1/2\,1/2\,\mathbf{c}_0}]$	${}_{0,2}[.\ n_{2,1}\ .\,.\,.]$	${}_{0,2}[n_{1,2}\ .\,.\,.\,.]$
${}_{0,1}[2\ .\ (\,.\,)\,.\,.]$ $[y = 1/4, z = 1/2]$	${}_{0,2}[\boldsymbol{t}_{1/2\,1/2\,\mathbf{c}_0}]$	${}_{0,2}[.\,.\,2_2\,.\,.]$	${}_{0,2}[n_{1,2}\ .\,.\,.\,.]$	${}_{0,2}[.\ n_{2,1}\ .\,.\,.]$
${}_{0,1}[\bar{1}]$ $[x = 0, y = 0, z = 1/2]$	${}_{0,2}[n_{1,2}\ .\,.\,.\,.]$	${}_{0,2}[.\ n_{2,1}\ .\,.\,.]$	${}_{0,2}[\boldsymbol{t}_{1/2\,1/2\,\mathbf{c}_0}]$	${}_{0,2}[.\,.\,2_2\,.\,.]$
${}_{0,1}[.\,.\,(a)\,.\,.]$ $[z = 1/2]$	${}_{0,2}[.\ n_{2,1}\ .\,.\,.]$	${}_{0,2}[n_{1,2}\ .\,.\,.\,.]$	${}_{0,2}[.\,.\,2_2\,.\,.]$	${}_{0,2}[\boldsymbol{t}_{1/2\,1/2\,\mathbf{c}_0}]$

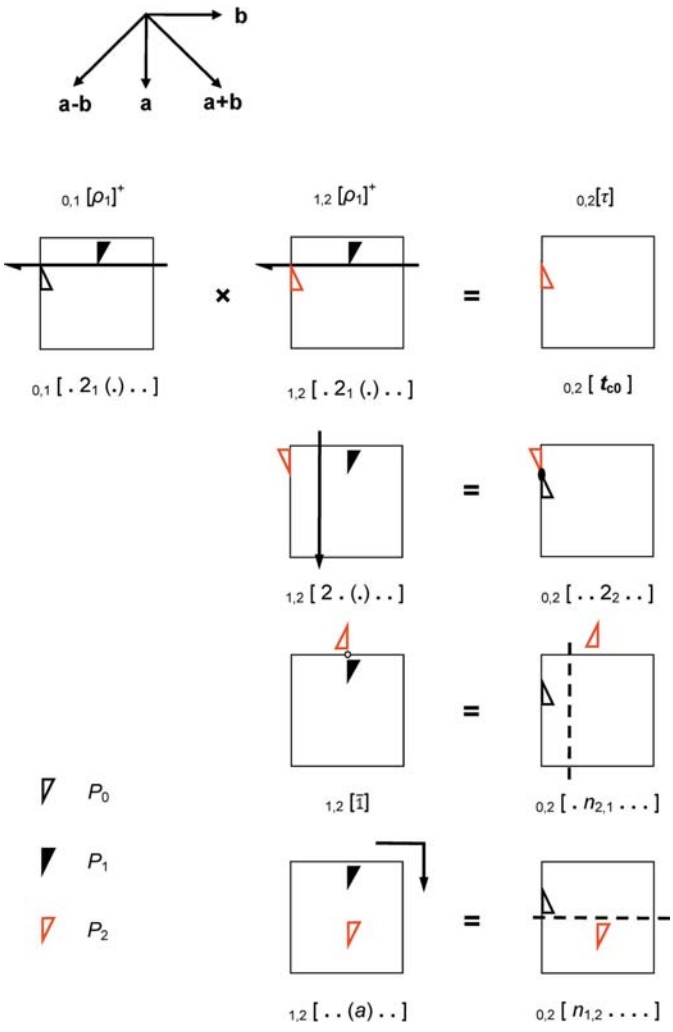

Figure 6
Graphical representation of the derivation of ${}_{0,2}[\tau]$ MDO-generating operations in the $1O$ polytype. The ${}_{0,1}[.\ 2_1\ (\,.\,)\,.\,.]^+$ PO (one of ${}_{0,1}[\rho_1]^+$ POs) is successively multiplied by all ${}_{1,2}[\rho_1]^+$ POs. For the sake of simplicity, only one of four wings of the symbolic figure is displayed. The packet P_2 is represented by the red empty figure in order to distinguish it from P_0. Similar pictures can be constructed for all three remaining ${}_{0,1}[\rho_1]^+$ POs.

(vii) Repeat the procedure for all remaining kinds of OD packets.

(viii) Check the list of MDO polytypes thus derived, and exclude redundant polytypes.

As mentioned above, there are four ${}_{0,1}[\rho]^+$ POs: ${}_{0,1}[.\ 2_1\ (\,.\,)\,.\,.]^+$, ${}_{0,1}[2\ .\ (\,.\,)\,.\,.]^+$ (congruent), ${}_{0,1}[\bar{1}]^+$, ${}_{0,1}[.\,.\,(a)\,.\,.]^+$ (enantiomorphous). The positions of the corresponding symmetry elements in the unit cell are indicated in Table 2, in square brackets below the symbols, and they are also apparent from Fig. 5(*b*). They represent one possible set of ${}_{0,1}[\rho]^+$ POs corresponding to one of two possible positions of P_1 with respect to P_0. These operations will be referred to as ${}_{0,1}[\rho_1]^+$ in the following.

The first possible triple is such that the packet P_2 is exactly above P_0 (sequence R • L R) and so are also the positions of symmetry elements for ${}_{1,2}[\rho_1]^+$ POs: ${}_{1,2}[.\ 2_1\ (\,.\,)\,.\,.]^+$, ${}_{1,2}[2\ .\ (\,.\,)\,.\,.]^+$, ${}_{1,2}[\bar{1}]^+$, ${}_{1,2}[.\,.\,(a)\,.\,.]^+$. Let us form all products ${}_{0,1}[\rho_1]^+ \cdot {}_{1,2}[\rho_1]^+ = {}_{0,2}[\tau]$. A graphical derivation of these products is illustrated in Fig. 6. In these pictures, only one of four 'wings' forming the symbolic figure is displayed. In this way the changes of orientation of the figure owing to the actions of consecutive POs can be more easily traced than for the complete figure. Note also that the wings are always oriented either as pointing up or down. This is because the whole symbolic figure cannot be generated solely by σ-POs but must be completed by local tetrads, λ-POs, of the packet.

Resulting operations transforming P_0 to P_2 are listed in Table 2. There are four ${}_{0,2}[\tau]$ operations altogether: ${}_{0,2}[\boldsymbol{t}_{\mathbf{c}_0}]$, ${}_{0,2}[.\,.\,2_2\,.\,.]$ (congruent), ${}_{0,2}[.\ n_{2,1}\ .\,.\,.]$, ${}_{0,2}[n_{1,2}\ .\,.\,.\,.]$ (enantiomorphous), and they all became total as MDO-generating τ-operations of the MDO1 polytype. All these operations contain the translational component $\mathbf{c}_0$ and the unit-cell vectors are **a**, **b**, $\mathbf{c}_0$. The total coincidence operations together with the ${}_{0,1}[\rho_1]^+$ operation related to **c** (${}_{1,2}[.\,.\,(a)\,.\,.]^+$) form the space group *Pbaa* (No. 54), Ramsdell's symbol of the polytype is $1O$. A projection of the polytype down **c** in the ball-and-stick model as well as symbolic figures with symmetry operations indicated is shown in Fig. 7(*a*). The side view of the structure is shown in Fig. 8(*a*). Its stacking symbol reads |R • L|. This polytype has really been found and corresponds to the structure described in the previous study (Hybler & Dušek, 2007).

The second possible triple contains the packet P_2 again above P_0, but in the second alternative orientation (the sequence R • L L). Therefore we have to take another set as ${}_{1,2}[\rho]^+$ POs: ${}_{1,2}[2_1\ .\ (\,.\,)\,.\,.]^+$, ${}_{1,2}[.\ 2\ (\,.\,)\,.\,.]^+$, ${}_{1,2}[\bar{1}]^+$, ${}_{1,2}[.\,.\,(b)\,.\,.]^+$. These operations are obtained as products of the POs from the previous set with certain λ-operations of the packet P_1 and they will be referred to as $[\rho_2]^+$ in the following. Positions of the respective symmetry elements are given in Table 3 in square brackets below the symbols. Note, that, for example, the position of ${}_{1,2}[\bar{1}]^+$ is different from ${}_{0,1}[\bar{1}]^+$. The resulting

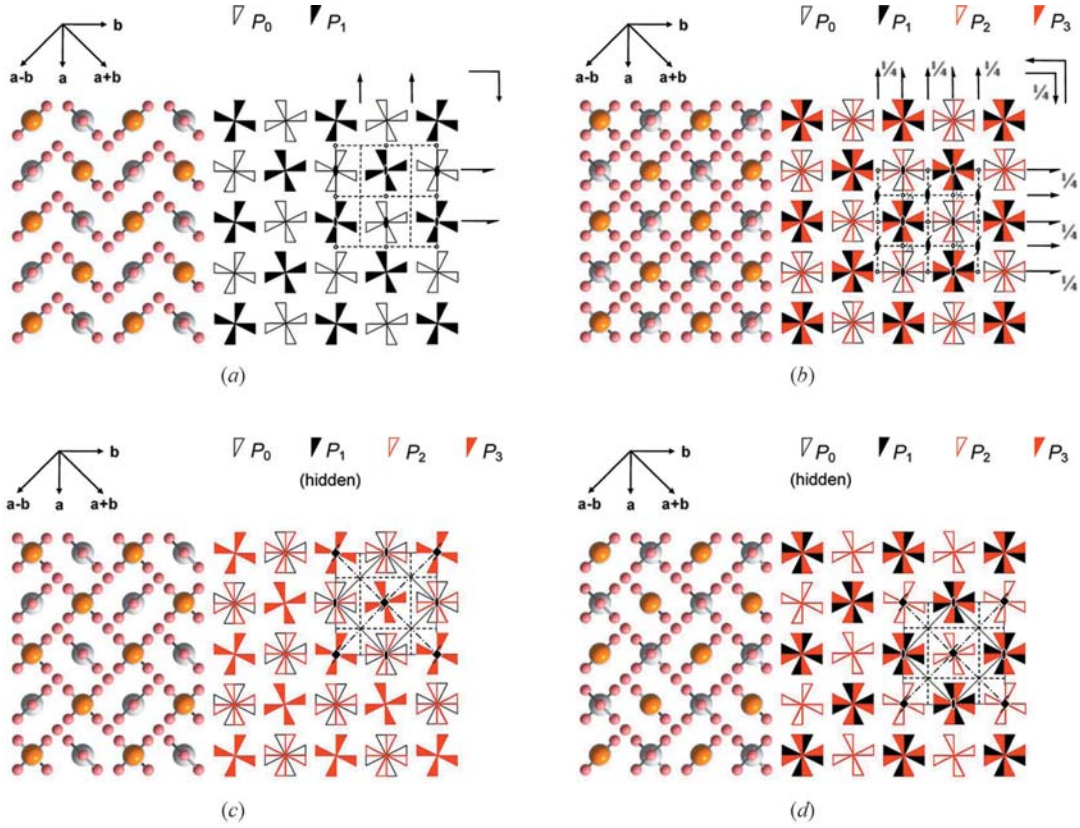

Figure 7
Two- and four-packet polytypes of kettnerite, projection down **c**, as a ball-and-stick model (left) and using symbolic figures (right). Symbolic figures of packets P_2 and P_3 (closer to the observer) are represented by the empty and full red figures, respectively, in order to distinguish them from P_0 and P_1. Symmetry elements of resulting space groups are indicated for one unit cell. Note the different origin required by the respective space groups of the polytypes. (*a*) Polytype 1*O* (MDO1), space group *Pbaa* (No. 54), lattice vectors **a**, **b**, $\mathbf{c}_0$. (*b*) Polytype 2*O* (MDO2), space group *Ibca* (No. 73), lattice vectors **a**, **b**, $2\mathbf{c}_0$. Right figures of P_2 superimpose the left figures of P_0 and *vice versa*; similarly the right figures of P_3 superimpose the left figures of P_1 and *vice versa*. In the ball-and-stick model, superimposed CO_3 groups of P_0 and P_2 as well as of P_1 and P_3 packets form diagonal crosses. (*c*) Polytype 2*Q* (non-MDO), space group $P4_2bc$ (No. 106), lattice vectors **a**, **b**, $2\mathbf{c}_0$. Right figures of P_2 superimpose the left figures of P_0 and left figures of P_2 superimpose the right figures of P_0. On the contrary, right figures of P_3 superimpose right figures of P_1 and left figures of P_3 superimpose left figures of P_1. Therefore the figures of P_1 are hidden behind those of P_3. In the ball-and-stick model, superimposed CO_3 groups of P_0 and P_2 form diagonal crosses, while superimposed CO_3 groups of P_1 and P_3 are parallel. (*d*) The same polytype 2*Q*, upside-down. In this case the right figures of P_3 superimpose the left figures of P_1 and the left figures of P_3 superimpose the right figures of P_1. The right figures of P_2 superimpose the right figures of P_0 and the left figures of P_2 superimpose the left figures of P_0. Therefore the figures of P_0 are hidden behind those of P_2. In the ball-and-stick model, superimposed CO_3 groups of P_1 and P_3 form diagonal crosses, while superimposed CO_3 groups of P_0 and P_2 are parallel.

products ${}_{0,1}[\rho_1]^+ \cdot {}_{1,2}[\rho_2]^+ = {}_{0,2}[\tau]$, coincidence operations transforming P_0 to P_2, are listed in Table 3, and their graphical derivation is shown in Fig. 9. Also, in this case there are four ${}_{0,2}[\tau]$: ${}_{0,2}[. \; . \; 2_2 \; . \; .]$, ${}_{0,2}[\boldsymbol{t}_{\frac{1}{2}\,\frac{1}{2}}\,\mathbf{c}_0]$ (congruent), ${}_{0,2}[. \; n_{2,1} \; . \; .]$ and ${}_{0,2}[n_{1,2} \; . \; . \; .]$ (enantiomorphous). These operations became total as MDO-generating τ-operations of the other MDO2 polytype. The ${}_{0,2}[\boldsymbol{t}_{\frac{1}{2}\,\frac{1}{2}}\,\mathbf{c}_0]$ operation generates the *I*-centred cell with unit-cell vectors **a**, **b**, $2\mathbf{c}_0$, Ramsdell's symbol is 2*O*. The ensemble of total coincidence operations together with the ${}_{0,1}[\rho_1]^+$ operation related to **c** (${}_{1,2}[. \; . \; (a) \; . \; .]^+$) forms the space group with symbol *Ibaa* (No. 73). However, following the recommendation in *International Tables for Crystallography* Volume A (2002), p. 60, the preferred space-group symbol *Ibca* should be used instead. Fig. 7(*b*) shows a projection of the polytype down **c** in the ball-and-stick model as well as symbolic figures with symmetry elements indicated. Fig. 8(*b*) displays the 2*O* polytype as a side view. The stacking symbol of the 2*O* polytype reads: |R • L L • R|. This polytype has not really been found to date.

It is also possible to determine a set of products ${}_{0,1}[\rho_2]^+ \cdot {}_{1,2}[\rho_2]^+ = {}_{0,2}[\tau]$. However, the resulting MDO-generating coincidence operations led again to the 1*O* polytype, but in an orientation turned by $\pi/2$ around **c**, with the permuted space-group symbol *Pbab*. In this case the stacking symbol reads |R • R|.

The stacking of packets in the two MDO polytypes can be also understood in the following way. In the MDO1, all packets P_{2n} exactly coincide in a projection down **c** and the same holds for all packets P_{2n+1}. On the other hand, in the MDO2, such a coincidence holds separately for all packets P_{4n}, P_{4n+1}, P_{4n+2} and P_{4n+3} (*cf.* Figs. 8*a* and 8*b*).

The procedures for the derivation of MDO polytypes described above exhaust all possibilities. No other MDO polytype thus exists in the family of kettnerite.

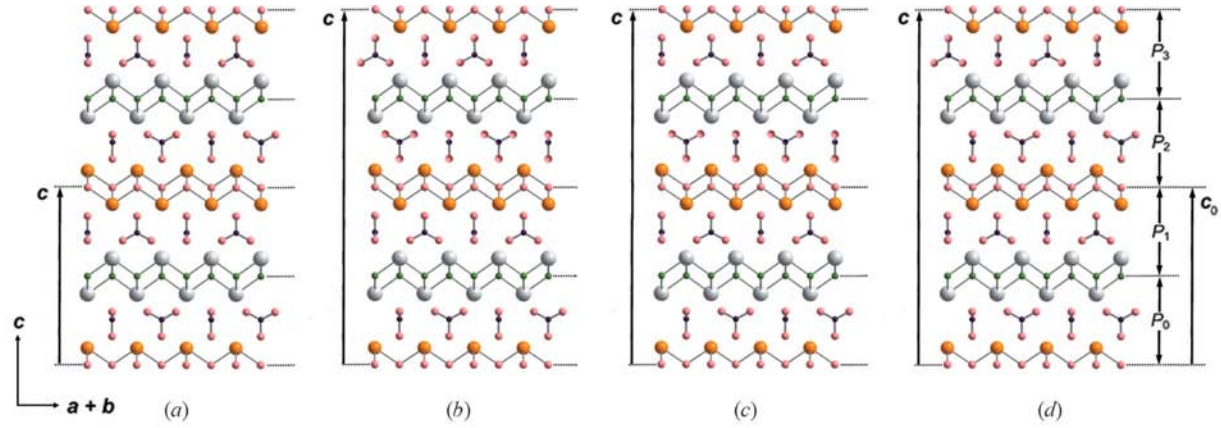

Figure 8
Two- and four-packet polytypes of kettnerite; slices parallel to the $(1\bar{1}0)$ plane of the larger cell (side view); ball-and-stick model. Four packets are displayed, as indicated on the right margin. Vectors **c** of all polytypes are indicated by arrows. (*a*) Polytype 1*O* (MDO1), lattice vectors **a**, **b**, $\mathbf{c}_0$. (*b*) Polytype 2*O* (MDO2), lattice vectors **a**, **b**, $2\mathbf{c}_0$. Note the opposite orientations of CO_3 groups in P_2 with respect to P_0, and in P_3 with respect to P_1 packets. (*c*) Polytype 2*Q*, lattice vectors **a**, **b**, $2\mathbf{c}_0$. Note the opposite orientation of CO_3 groups in P_2 with respect to P_0, and the same orientation of them in P_1 and P_3 packets. (*d*) Polytype 2*Q*, upside-down, **a**, **b**, $2\mathbf{c}_0$. Note the opposite orientation of CO_3 groups in P_3 with respect to P_1, and the same orientation of them in P_0 and P_2 packets.

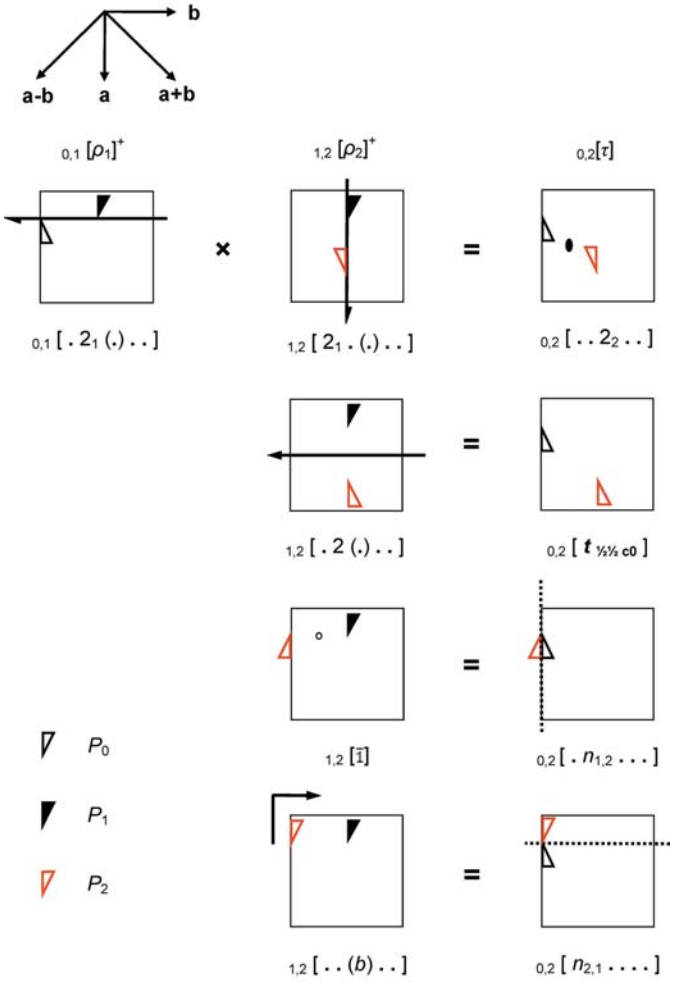

Figure 9
Graphical representation of the derivation of $_{0,2}[\tau]$ MDO-generating operations in the 2*O* polytype. The $_{0,1}[.\ 2_1\ (\ .\ )\ .\ .]^+$ PO (one of $_{0,1}[\rho_1]^+$ POs) is successively multiplied by all $_{1,2}[\rho_2]^+$ POs. Similar pictures can be constructed for all three remaining $_{0,1}[\rho_1]^+$ POs.

3.5. A peculiar hypothetical non-MDO polytype

The stacking rules described above might result in peculiar stacking sequences. As an example, we can use a non-MDO polytype with doubled repeat unit (cell parameters **a**, **b**, $2\mathbf{c}_0$), shown in Figs. 7(*c*) (down **c**) and 8(*c*) (side view). Its stacking symbol reads

$$|\mathrm{R}\ \bullet\ \mathrm{L}\quad \mathrm{L}\bullet\ \mathrm{L}|.$$

In this polytype, all packets P_{2n+1} exactly coincide in a projection down **c**, while the coincidence holds separately for P_{4n} and P_{4n+2}. The P_{4n} packets are mapped onto the P_{4n+2} packets by 4_4 screw rotations (recall that the screw component is related to $\mathbf{c}_0$) around the axes located in the local tetrads of odd packets. These screw rotations are also valid for odd packets, but they do not change the orientation of P_{2n+3} with respect to P_{2n+1}. In the doubled cell the screw axis symbol is 4_2 and the corresponding coincidence operation becomes total for the polytype. The resulting symmetry is $P4_2bc$ (No. 106), the polytype is really tetragonal, and Ramsdell's symbol is 2*Q*. The symmetry elements are indicated in Fig. 7(*c*). It is worth noting that the structure as a whole is polar.

The stacking symbol: $|\mathrm{R}\bullet\mathrm{L}\quad\mathrm{R}\bullet\mathrm{R}|$ represents the same polytype turned upside-down. In this case, all packets P_{2n} exactly coincide in a projection down **c**, while the coincidence holds separately for P_{4n+1} and P_{4n-1} [*cf.* Figs. 7(*d*) and 8(*d*)]. This polytype remains hypothetical to date.

3.6. Stacking faults, out-of-step domains and twins

The present considerations assumed regular stacking sequences in periodic polytypes. However, the diffuseness of polytype reflections in the X-ray pattern proved a strong tendency in kettnerite to disordering. Therefore various possibilities of disordering should be discussed as well.

Table 4
Stacking sequences of possible domains of polytypes 1*O*, 2*O* and 2*Q*.

Polytype	Initial sequence	(**a** + **b**)/2 shifted	$\pi/2$ rotated	$\pi/2$ rotated and (**a** + **b**)/2 shifted
1*O*	|R • L|	|L • R|	|R • R|	|L • L|
2*O*	|R • L L • R|	|L • R R • L|	|R • R L • L|	|L • L R • R|
2*Q*	|R • L L • L|	|L • R R • R|	|R • R L • R|	|L • L R • L|
2*Q* upside-down	|R • R R • L|	|L • L L • R|	|R • L R • R|	|L • R L • L|

An 'improper' position of one packet in an otherwise regular sequence causes an isolated *stacking fault*. It can be, for example, expressed as follows (in the 1*O* polytype),

R • L R • L R • R R • L R • L R • L
↑
stacking fault

If some portion of an otherwise regular sequence is shifted as a whole by (**a** + **b**)/2, an *out-of-step domain* is produced. As a result of the transformation the orientational characters in both kinds of packets are interchanged with respect to the rest of the sequence. An example of the sequence with an out-of-step domain of the 1*O* polytype reads

R • L R • L R • L R • R L • R L • R L • R
↑
out-of-step domain boundary

With respect to the given coordination system, the stacking rule allows existence of two kinds of domains mutually shifted by (**a** + **b**)/2.

For the 2*O* polytype, an example of a sequence with out-of-step domain reads

R • L L • R R • L L • R L • R R • L L • R R • L
↑
out-of-step domain boundary

and for the 2*Q* polytype,

R • L L • L R • L L • L L • R R • R L • R R • R
↑
out-of-step domain boundary

Another kind of domain is produced if some portion of the structure is rotated by $\pi/2$ around local tetrads. This operation changes orientational characters in packets of one parity (say even), and leaves unchanged those of the other parity (say odd). This gives rise to a twin domain, and $\pi/2$ rotation, corresponding to [. . (4^1) . .] λ operation of, say, even packets, serves as a twin operation. For the 1*O* polytype, the sequence with the twin domain reads, for example,

R • L R • L R • L R • R R • R R • R R • R
↑
twin boundary

The arrangement of atoms or symbolic figures in the second twin individual corresponds to the images in Figs. 5(*b*) and 7(*a*) rotated by $\pi/2$ while the coordinate system remains unchanged. However, within the second twin individual, out-of-step domains shifted by (**a** + **b**)/2 are possible too. These domains are alternatively obtained by the $\pi/2$ rotations, around tetrads of odd packets. Therefore four kinds of domains altogether can exist within the polytype 1*O*. An example of a sequence containing all possible domains reads

R • L R • L R • R L • R L • R R • R R • R R • L L • L L • L
↑ ↑ ↑
domain boundary twin boundary domain boundary

This twinning really exists and the structure of the 1*O* polytype was actually refined as twin (Hybler & Dušek, 2007). In that paper, four kinds of packet pairs (double packets) were derived. The domains mentioned above are obtained by repeated stacking of these packet pairs.

In the polytype 2*O*, four similar kinds of domains can be derived. The polytype 2*Q*, because of its polar character, allows the existence of another upside-down domain. They correspond to structures displayed in Figs. 7(*c*) and 8(*c*) and Figs. 7(*d*) and 8(*d*) co-existing in one crystal. Combining with domains already defined, eight kinds of domains can exist in this polytype. The upside-down operation can of course be applied to 1*O*, and 2*O* polytypes as well, but in this case it provides sequences that are either identical to the initial ones, or to those obtained by the (**a** + **b**)/2 shift. Sequences corresponding to all domains allowed by the stacking rule for 1*O*, 2*O* and 2*Q* polytypes are summarized in Table 4. According to this table, there are 16 kinds of domains altogether.

In the polytype 2*O*, the sequence corresponding to the (**a** + **b**)/2 shift can be alternatively obtained by cyclic permutation of packet pairs [*cf.* initial and (**a** + **b**)/2 shifted sequences in Table 4]. In the 2*Q* polytype, the sequences permuted in the same way correspond to those obtained by the $\pi/2$ rotations. Therefore, in this polytype the $\pi/2$ rotation does not produce a twin, but rather out-of-step domains.

A tentative derivation of sequences corresponding to all possible kinds of domains of theoretically possible six-packet polytypes was also performed. To all sequences of four packets, and doubled sequences of packet pairs of the 1*O* polytype (*cf.* Table 4), additional packet pairs of four possible kinds were added. The 64 six-packet sequences generated in this way are listed in Table 5. The sequences in the first line belong to the 1*O* polytype, as they contain repetitions of three identical pairs. The remaining 60 sequences were checked for equivalency by application of all allowed operations: (**a** + **b**)/2 translations, $\pi/2$ rotations and turning upside-down. All possible cyclic permutations of packet pairs were also considered. Thus, for example, the sequence |R • R L • L R • R| has permuted equivalents |L • L R • R R • R| and |R • R R • R L • L|. In this way it was revealed that all sequences belonged to only four

Table 5
Stacking sequences of possible domains of six-packet polytypes of kettnerite.

The sequences in the first line represent those of the 1*O* polytype three times repeated. Otherwise the stacking rule allows four polytypes (numbered) in 60 domains.

Initial	(**a** + **b**)/2 shifted	π/2 rotated	π/2 rotated and (**a** + **b**)/2 shifted	Polytype
|R • L R • L R • L|	|L • R L • R L • R|	|R • R R • R R • R|	|L • L L • L L • L|	1*O*
|R • L R • L L • R|	|L • R L • R R • L|	|R • R R • R L • L|	|L • L L • L R • R|	1
|R • L R • L L • L|	|L • R L • R R • R|	|R • R R • R L • R|	|L • L L • L R • L|	2
|R • L R • L R • R|	|L • R L • R L • L|	|R • R R • R R • L|	|L • L L • L L • R|	2
|R • L L • R R • L|	|L • R R • L L • R|	|R • R L • L R • R|	|L • L R • R L • L|	1
|R • L L • R L • R|	|L • R R • L R • L|	|R • R L • L L • L|	|L • L R • R R • R|	1
|R • L L • R L • L|	|L • R R • L R • R|	|R • R L • L L • R|	|L • L R • R R • L|	3
|R • L L • R R • R|	|L • R R • L L • L|	|R • R L • L R • L|	|L • L R • R L • R|	4
|R • L L • L R • L|	|L • R R • R L • R|	|R • R L • R R • R|	|L • L R • L L • L|	2
|R • L L • L L • R|	|L • R R • R R • L|	|R • R L • R L • L|	|L • L R • L R • R|	4
|R • L L • L L • L|	|L • R R • R R • R|	|R • R L • R L • R|	|L • L R • L R • L|	2
|R • L L • L R • R|	|L • R R • R L • L|	|R • R L • R R • L|	|L • L R • L L • R|	3
|R • L R • R R • L|	|L • R L • L L • R|	|R • R R • L R • R|	|L • L L • R L • L|	2
|R • L R • R L • R|	|L • R L • L R • L|	|R • R R • L L • L|	|L • L L • R R • R|	3
|R • L R • R L • L|	|L • R L • L R • R|	|R • R R • L L • R|	|L • L L • R R • L|	4
|R • L R • R R • R|	|L • R L • L L • L|	|R • R R • L R • L|	|L • L L • R L • R|	2

distinct polytypes. As they were not a matter of further studies, they were only numbered and these numbers are indicated in respective lines in Table 5.

4. Desymmetrization

The present considerations assumed an idealized model of OD layers and packets in kettnerite. The refinement of the polytype 1*O* revealed certain displacements of O1 and F1 atoms from ideal positions as well as slight ($\sim$4°) rotation of CO_3 groups (Hybler & Dušek, 2007). These changes can be easily explained as a result of repulsive forces of anions. Especially prone to these changes are F1 and O3 atoms (belonging to the CO_3 groups), because of their relative proximity. However, the nature of these changes is such that they do not affect the space-group symmetry *Pbaa* of the polytype 1*O*. For other possible polytypes no experimental results are available, therefore the desymmetrization is not further discussed in this study.

5. Conclusion

This study presents a description of a new family of OD structures. The MDO and some non-MDO polytypes are derived and possible kinds of domains discussed. However, the real existence of periodic polytypes with more than two packets per period seems improbable as it requires a long-range order over a relatively long distance. Moreover, the experimental studies revealed a strong tendency in kettnerite to disordering. Despite these stipulations, the study is presented as a certain kind of exercise in the application of the OD theory.

We thank the National Museum in Prague and particularly the private collector M. Zeman from Jičín, Czech Republic, for providing samples used for structure determination. We also thank Dr Libuše Jilemnická for critically reading the text. Suggestions and comments of two anonymous referees are highly appreciated. The study has been supported by the grant 205/07/0302 of the Czech Science Foundation.

References

Aurivillius, B. (1949*a*). *Ark. Kemi*, **1**, 463–480.
Aurivillius, B. (1949*b*). *Ark. Kemi*, **1**, 499–512.
Aurivillius, B. (1950). *Ark. Kemi*, **2**, 519–527.
Dornberger-Schiff, K. (1956). *Acta Cryst.* **9**, 593–601.
Dornberger-Schiff, K. (1964). *Chem. Geol. Biol.* **3**, 1–107.
Dornberger-Schiff, K. (1966). *Lehrgang über OD-Strukturen.* Akademie Verlag Berlin.
Dornberger-Schiff, K. & Grell, H. (1982). *Acta Cryst.* A**38**, 491–498.
Ďurovič, S. (1974). *Acta Cryst.* B**30**, 76–78.
Ďurovič, S. (1979). *Krist. Tech.* **14**, 1047–1053.
Ďurovič, S. (1997). *Modular Aspects of Minerals*, edited by S. Merlino, pp. 1–28. Budapest: Eötvös University Press.
Ďurovič, S. (1999). *International Tables for Crystallography*, Vol. C, 2nd ed., edited by A. J. C. Wilson & E. Prince, §9.2. Dordrecht: Kluwer Academic Publishers.
Grell, H. & Dornberger-Schiff, K. (1982). *Acta Cryst.* A**38**, 49–54.
Hybler, J. & Dušek, M. (2007). *Eur. J. Mineral.* **19**, 411–418.
International Tables for Crystallography. (2002). Vol. A, 5th ed., edited by Th. Hahn. Dordrecht: Kluwer Academic Publishers.
Lagercrantz, A. & Sillén, L. G. (1948). *Ark. Kemi Mineral. Geol.* **25**A, 1–21.
Syneček, V. & Žák, L. (1960). *Czech. J. Phys.* B**10**, 195–207.
Weiss, Z. & Ďurovič, S. (1980). *Acta Cryst.* A**36**, 633–640.
Žák, L. & Syneček, V. (1956). *Čas. Min. Geol.* **1**, 195–197.
Žák, L. & Syneček, V. (1957). *University Carol. Geol.* **3**, 1–46.